Complex modal analysis of a vertical rotor through finite element method

C.E. Agostini and E.A. Capello Sousa

Department of Mechanical Engineering, Unesp - State University of São Paulo, Bauru, SP, Brazil, 55 (14) 3234-1108.
Department of Mechanical Engineering, Unesp - State University of São Paulo, Bauru, SP, Brazil.

Natural frequencies were analyzed (axial, torsional and flexural) and frequency response of a vertical rotor with a hard disk at the edge through the classical and complex modal analysis. The mathematical modeling was based on the theory of Euler-Bernoulli beam. The equation that rules the movement was obtained through the Lagrangian formulation. The model considered the effects of bending, torsion and axial deformation of the shaft, besides the gravitational and gyroscopic effects. The finite element method was used to discretize the structure into hollow cylindrical elements with 12 degrees of freedom. Mass, stiffness and gyroscopic matrices were explained consistently. This type of tool, based on the use of complex coordinates to describe the dynamic behavior of rotating shaft, allows the decomposition of the system in two submodes, backward and forward. Thus, it is possible to clearly visualize that the orbit and direction of the precessional motion around the line of the rotating shaft is not deformed. A finite element program was developed using Matlab ®, and numerical simulations were performed to validate this model.

Keywords: Finite Elements, Rotor Dynamics, Modal Analysis, Drill string Vibrations.

INTRODUCTION

Rotary machines are mechanical systems that have several applications, such as engines and electrical generators, hydraulic turbines, pumps, compressors, wellbore construction and others.

The dynamic behavior of a mechanical system must be examined in its design phase so that you can determine whether it will present a satisfactory performance or not in its condition of the planned operation. The natural frequencies, damping factors and vibration modes of these systems can be analytically, numerically or experimentally determined.

The study for rotary machines, however, requires a more careful and detailed analysis, because the rotation movement of the rotor significantly influences the dynamic comportment of the system, making the model parameters dependent on the rotation of the machine.

The gyroscopic effect couples the rotation movement and, as it's known, it is dependent on the rotation speed of the rotor. Therefore, it is expected that the natural frequencies and vibration modes of a rotating machine also depend on the system speed.

In this case, the so called precession modes arise, where the mass or geometrical center of each cross section of the rotor describes orbits around the line connecting them. The rotor presents a rotation that is the composition of two overlapping responses: a rotor rotation around itself and the rotating shaft flexed around its non deflected setting. The orbit can be described in the same direction as the self rotation, constituting itself in the so-called forward whirl, or it may have opposite direction, being named as backward whirl Souto (2000).

It is then observed that in the presence of the gyroscopic effect matrix, the own speed of the rotor affects the value of the natural frequencies of the system. This fact explains the relation between natural whirl frequencies and rotation of the rotor itself, represented by the Campbell diagram. The skew-symmetric shape of the gyroscopic matrix implies in 2n distinct natural frequencies for each shaft speed rotation, a larger and

another smaller one from each of the n natural frequencies of the system without rotation, generally corresponding to backward and forward modes da Silva (2004).

Currently there are many studies regarding to the study of vibrations in rotating shafts, mainly in oil wells drilling, where the vibration problems in the drill string cause poor performance in penetration rate, shortening the lifetime of the bits, mechanical stress in the pipes, unexpected changes in the direction of drilling, besides the equipment failure in geosteering and geological mapping.

Mathematical models have been evolving for decades, and one of the most powerful tools of numerical analysis, the finite element method, has performed a decisive role in the investigation of rotating mechanical systems.

In its work on vertical rotors Dana (1987), it analyzes a stationary vertical rotor and, through the FEM, predicts the eigen values of rotating systems and discusses the effects of forward and backward whirl. An adaptation of previous FEM software for analysis of simple drill string, including nonlinear analysis is used in Cordovil (1991). Both works, however, does not include gyroscopic and gravitational effects in the structure.

Drillstring can be analyzed as a vertical rotary axis in balance where three types of vibration can be experienced: axial, torsional and lateral vibration.

An overall dynamic analysis of drill string is often complicated because the three types of vibration listed previously above may be present, at same time, as well as disorders associated with each type of vibration: forward and backward whirl associated with lateral vibration, stick-slip associated with torsional vibration and bit-bounce associated with the axial vibration, Alamo (2003).

In Axisa et al. (1990), it is presented a dynamic model using FEM which includes the effect of bending and torsion, but these are treated in an uncoupled way. In Dunayevsky et al. (1993), it is employed the use of FEM in a model to calculate the modal characteristics in drill strings, however, the model is limited to parametric resonance vibrations evenly distributed in beams supported on the edges. In this case, as in previous work, the formulations do not deal with gravity and gyroscopic effects in these structures.

The tool of classical modal analysis provides reliable results in stationary structures and has been widely used for this purpose. In the case of rotating machines, this kind of approach involves a series of limitations as for its use in determining the vibration characteristics of the system Ewins (1998).

The use of modal analysis on rotating machinery requires a more rigorous theoretical improvement. This is basically due to the spin effect on which the structure is subjected. The fact of the rotation existence in the structure causes to emerge on the system the so called Coriolis acceleration due to rotation of the rotor around another axis, than the rotation itself. These accelerations lead to the rise of gyroscopic forces.

The technique of complex modal analysis was developed by Lee (1991). The work of Kessler (1999) and Souto (2000), deal with the methodology of the technique in a more understandable way, with examples and applications, however, the approach is more superficial. Basically the methodology consists in using complex coordinates to describe the node movement of the structure. This new coordinate system allows to incorporate the directionality of the modes or dismember them in two sub-modes (forward and backward whirl). This is one of the advantages of this methodology, where the identification of the whirl movement is a very important step in the analysis of a rotating machine because these movements directly affect the lifespan of the rotor.

The proposed work is about the implementation, in a MATLAB ® environment, of a finite elements system for calculating the natural frequencies and hence obtaining Campbell diagrams and charts to complex modal analysis of rotating shafts subjected to gyroscopic and gravitational effects.

In this paper, the finite element method is employed for modeling rotating vertical tubular structures with 12 degrees of freedom at each node, using elements of 3D Euler-Bernoulli beams type.

The gyroscopic and gravitational effects are considered in the model. The implementation in MATLAB ®, allows the input and output data to be properly modified to other types of structures and analysis.

The natural axial, torsional and transverse frequencies may be obtained as well as Campbell diagrams, graphs with complex and traditional modal analysis. Comparisons are made between the complex and classical modal analysis, focusing on the easiness of whirl modes observation, since the complex modal analysis allows clear distinction in separate curves for the forward and backward whirl mode.

Mathematical modeling

Basic concepts

This present formulation was based on the work of Alnaser (2002), Bazoune et al. (2001) and Khulief et al. (1997) and considers the following hypothesis: linear, homogeneous and isotropic elastic material, axi-symmetric rotor and, besides, shifts refer to the central axis line of the component and the damping structure was disregarded. Figure 1 illustrates the coordinate system adopted for the rotation system modeling. The XYZ axis refer to the undeformed system and the xyz axis system after the deformation of the element

The xyz coordinate system is rotated in relation to the XYZ system according to the set of angles shown in Fig-

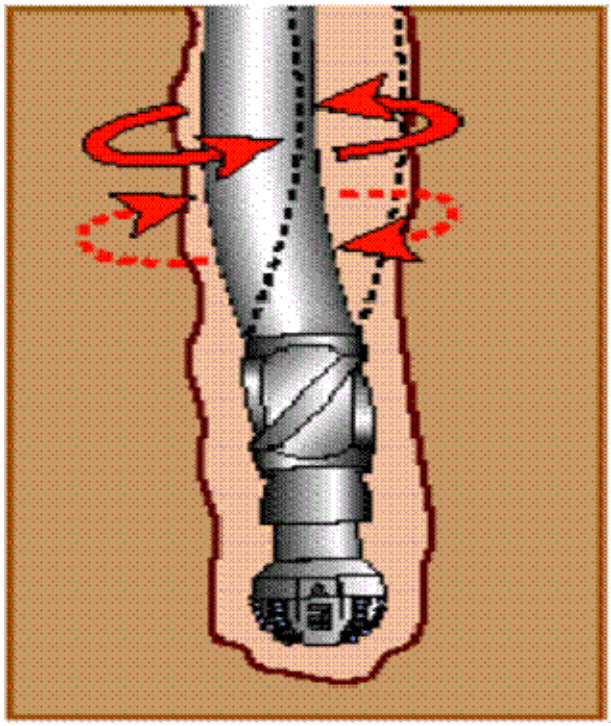

Figure 1. Schematic drillstring, Bashmal (2004).

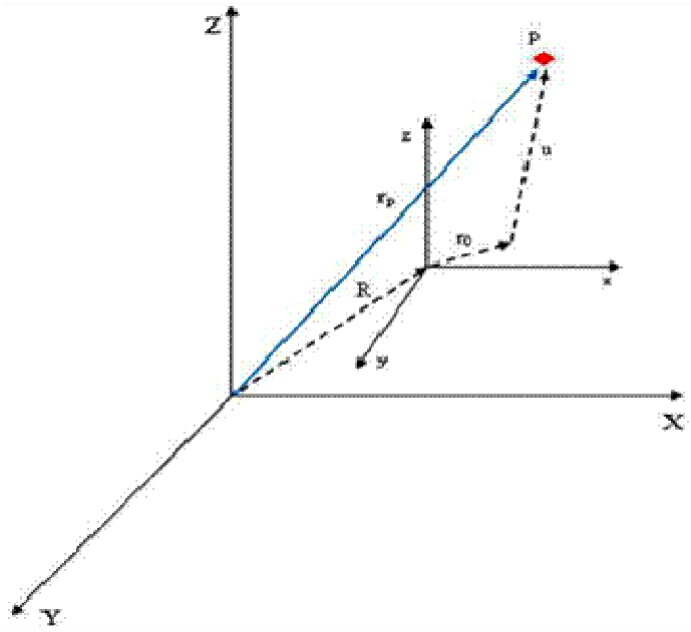

Figure 2. Generalized coordinates system.

ure 2, where the general orientation of the cross section of the beam element can be obtained by rotation around the X axis with angle φ, then by an angle θ_y around the new axis y_1 and subsequently by an angle θ_z around the final shaft z_2.

The instantaneous angular speed ω, related to the coordinate system xyz, can be seen in (1).

$$\omega = \dot{\phi}\, i + \dot{\theta}_y\, j_1 + \dot{\theta}_z\, k_2 \quad (1)$$

Where: i, j_1 and k_2 are the unit vectors along the axis x, y_1 and z_2.

Transforming (1) for the XYZ coordinate system and assuming small angles to θ_y and θ_z will yield:

$$\omega = \begin{Bmatrix} \omega_X \\ \omega_Y \\ \omega_Z \end{Bmatrix} = \begin{bmatrix} \dot{\varphi} - \dot{\theta}z\ \theta y \\ \dot{\theta}y \cos\varphi - \dot{\theta}z\ \sin\varphi \\ \dot{\theta}z\ \cos\varphi + \dot{\theta}y\ \sin\varphi \end{bmatrix} \quad (2)$$

Adopting p, shown in Fig. 1, as any point in the undeformed position of the beam and defining the vector r_p with respect to global coordinate system XYZ, will yield:

$$r_p = R + r_0 + u \quad (3)$$

Where u is the deformation vector at point p. Using finite element analysis, u can be written:

$$u = [N_t]\{e\} \quad (4)$$

Where $[N_t]$ is the function form matrix for the 3D beam element and the vector $\{e\}$ contains the nodal displacements of the element, according to (5).

$$e = \{u_1\ v_1\ w_1\ \ \theta_{y_1}\ \ \theta_{z_1}\ \varphi_1\ u_2\ v_2\ w_2\ \theta_{y_2}\ \theta_{z_2}\ \varphi_2\}^T \quad (5)$$

The deformations due to the translation effect of the elements in terms of functions of form are:

$$\begin{Bmatrix} u(x,t) \\ v(x,t) \\ w(x,t) \end{Bmatrix} = \begin{bmatrix} N_{u_1} & 0 & 0 & 0 & 0 & 0 & N_{u_2} & 0 & 0 & 0 & 0 & 0 \\ 0 & N_{v_1} & 0 & 0 & N_{v_2} & 0 & 0 & N_{v_3} & 0 & 0 & N_{v_4} & 0 \\ 0 & 0 & N_{v_1} & N_{v_2} & 0 & 0 & 0 & 0 & N_{v_3} & -N_{v_4} & 0 & 0 \end{bmatrix} = \begin{bmatrix} N_u \\ N_v \\ N_w \end{bmatrix} \{e\} = [N_t(x)]\{e(t)\} \quad (6)$$

The rotation of the elastic element can be approximated by:

$$\begin{Bmatrix} \theta_y \\ \theta_z \end{Bmatrix} = \begin{bmatrix} 0 & N_{\theta_1} & 0 & 0 & N_{\theta_2} & 0 & 0 & N_{\theta_3} & 0 & 0 & N_{\theta_4} & 0 \\ 0 & 0 & -N_{\theta_1} & N_{\theta_2} & 0 & 0 & 0 & 0 & -N_{\theta_3} & N_{\theta_4} & 0 & 0 \end{bmatrix} = \begin{bmatrix} N_{\theta_y} \\ N_{\theta_z} \end{bmatrix} \{e\} = [N_\theta(x)]\{e(t)\} \quad (7)$$

Torsional deformation is given by (8):

$$\varphi(x,t) = [0\ 0\ 0\ 0\ 0\ N_{\varphi_1}\ 0\ 0\ 0\ 0\ 0\ N_{\varphi_2}]\ e = [N_\varphi]\{e(t)\} \quad (8)$$

The derivative with respect to time of (3) can be expressed as:

$$\frac{dr_p}{dt} = r_p' + \omega \times r_p = r_p' + [\omega]\{r_p\} \quad (9)$$

Where the matrix $[\omega]$ is anti-symmetric (3 x 3) associated with the rotational vector ω.

$$[\omega] = \begin{bmatrix} 0 & -\omega_z & \omega_y \\ \omega_z & 0 & -\omega_x \\ -\omega_y & \omega_x & 0 \end{bmatrix} \quad (10)$$

Since the magnitude of R and r_0 do not vary with the deformation of the element, will yield:

$$r_p' = \dot{u} = [N_t]\{\dot{e}\} \quad (11)$$

Substituting (11) in (9):

$$\frac{dr_p}{dt} = [N_t]\{\dot{e}\} + [\omega]\{r_p\} \quad (12)$$

Kinetic energy

The expression for the kinetic energy of the element can be written as:

$$T = \frac{1}{2}\int_V \mu \left\{\frac{dr_p}{dt}\right\}^T \left\{\frac{dr_p}{dt}\right\} dV \quad (13)$$

Where μ is the mass specific of the element. Substituting (12) in (13):

$$T = \frac{1}{2}\int_V \mu \left[\{\dot{e}\}^T [N_t]^T [N_t]\{\dot{e}\} + \{\dot{e}\}^T [N_t]^T [\omega]\{r_p\} + \{r_p\}^T [\omega]^T [N_t]\{\dot{e}\} + \{r_p\}^T [\omega]^T [\omega]\{r_p\}\right] dV \quad (14)$$

The second and third terms of (14) are equally zero, because the moment of inertia is calculated with respect to the center of mass of the element. The first term represents the kinetic energy due to the translation effect and the last term the kinetic energy due to the rotational effect, already including the gyroscopic effects. After algebraic manipulations, one gets at the expression of kinetic energy, as shown in (15).

$$T = \frac{1}{2}\{\dot{e}\}^T [M_t]\{\dot{e}\} + \frac{1}{2} C\dot{\varphi}^2 + \{\dot{e}\}^T [M_\varphi]\{\dot{e}\} - \dot{\varphi}\{\dot{e}\}^T [G]\{\dot{e}\} - \{\dot{e}\}^T [M_e]\{\dot{e}\} + \{\dot{e}\}^T [M_r]\{\dot{e}\} \quad (15)$$

Where:

$$[M_t] = \int_0^l [N_v]^T \mu A [N_v] dx \quad (16)$$

$$[M_r] = \int_0^l [N_\theta]^T I_D [N_\theta] dx \quad (17)$$

$$[M_\varphi] = \int_0^l [N_\varphi]^T I_P [N_\varphi] dx \quad (18)$$

$$[M_e] = \int_0^l I_P \begin{pmatrix} [N_\varphi]^T [N_{\theta_z}]\{e\}[N_{\theta_y}] \\ -[N_\varphi]^T [N_{\theta_y}]\{e\}[N_{\theta_z}] \end{pmatrix} dx \quad (19)$$

$$G = [G^*] - [G^*]^T \quad (20)$$

$$[G^*] = \int_0^l I_P [N_{\theta_y}][N_{\theta_z}] dx \quad (21)$$

$$C = \int_0^l I_P\, dx \quad (22)$$

Where:

I_P polar mass moment of inertia and I_D the diametral mass moment of inertia, according to (23) and (24).

$$I_D = \mu I_y = \mu I_Z \quad (23)$$

$$I_P = \mu I_X \quad (24)$$

Thus (15) can be written in a compact matrix form as seen in (25).

$$T = \frac{1}{2}\{\dot{e}\}^T [M]\{\dot{e}\} + \frac{1}{2} C\dot{\varphi}^2 + \dot{\varphi}\{\dot{e}\}^T [G]\{\dot{e}\} \quad (25)$$

$$M = [M_t] + [M_r] + [M_\varphi] - 2[M_e] \quad (26)$$

M is the augmented mass matrix of the 3D beam element; where $[M_e]$ is the coupled torsional-transverse mass matrix, which will be ignored in this paper, since it is dependent on time; $[M_t]$ is the translation mass matrix; $[M_r]$ is the rotary inertia mass matrix e $[M_\varphi]$ is the torsional mass matrix.

Strain energy

Adopting for the 3D beam element the variables (u, v, w) as deformation of translation, one axial and two bending, and the variables (θ_y , θ_z , φ) composed of two deformation, one related to bending and another with torsion, the equation of the elastic strain energy for combined axial deformation, bending and torsion can be written as (27).

$$U_{elast} = \frac{1}{2}\int_0^l \left[EA\left(\frac{du}{dx}\right)^2 + EI_z\left(\frac{\partial^2 v}{\partial x^2}\right)^2 + EI_y\left(\frac{\partial^2 w}{\partial x^2}\right)^2 + GJ\left(\frac{\partial \varphi}{\partial x}\right)^2 \right] dx \quad (27)$$

The result considering the strain energy due to the gravitational effect is:

$$U_{gravit} = \frac{1}{2}\int_0^l F(x)\left[\left(\frac{\partial w}{\partial x}\right)^2 + \left(\frac{\partial v}{\partial x}\right)^2\right] dx \quad (28)$$

Where $F(x)$ is the gravitational force given by (29).

$$F(x) = EA\frac{\partial u}{\partial x} \quad (29)$$

Adding portions of strain energy and considering the symmetrical cross section, that is, $I_z = I_y = I(x)$, will

yield:

$$U = \frac{E}{2}\int_0^l I(x)\left[\left(\frac{\partial\theta_y}{\partial x}\right)^2 + \left(\frac{\partial\theta_x}{\partial x}\right)^2\right]dx + \frac{EA}{2}\int_0^l \left(\frac{du}{dx}\right)^2 dx + \frac{GJ}{2}\int_0^l \left(\frac{d\varphi}{dx}\right)^2 dx + \frac{1}{2}\int_0^l F(x)\left[\left(\frac{\partial w}{\partial x}\right)^2 + \left(\frac{\partial v}{\partial x}\right)^2\right]dx$$

(30)

Writing (30) in matrix form will yield:

$$U = \frac{1}{2}\{e\}^T[K]\{e\} \quad (31)$$

$$K = [K_a] + [K_b] + [K_\varphi] + [K_g] \quad (32)$$

K is the augmented stiffness matrix of the 3D beam element; where $[K_a]$ is the axial stiffness matrix, $[K_b]$ is the elastic stiffness matrix, $[K_\varphi]$ is the torsional stiffness matrix and $[K_g]$ is the axial stiffening matrix due to gravitational effect (pipe under tension).

Equation of motion

The expression for the movement of the mechanical system is derived by Lagrange equation (33).

$$\frac{d}{dx}\left(\frac{\partial L}{\partial \dot{q}}\right) - \frac{\partial L}{\partial q} = Q \quad (33)$$

Where:

$L = T - U$	Lagrangian function
q	Generalized coordinates
Q	Vector of generalized forces
T	Total kinetic energy
U	Total strain energy

Substituting q and L in (33) it is obtained the finite element formulation for the dynamics of movement given by (34).

$$[M]\{\ddot{e}\} + \dot{\varphi}[G]\{\dot{e}\} + [K]\{e\} = \{Q\} \quad (34)$$

Where:

$[M]$	Augmented mass matrix
$[G]$	Gyroscopic matrix
$[K]$	Augmented stiffness matrix
$\dot{\varphi}$	Angular velocity

Complex modal analysis

Adopting p(t) as the complex vector that relates the real coordinates y(t) and z(t) results in:

$$p(t) = y(t) + iz(t) \quad (35)$$

Expanding y(t) e z(t) in Fourier series will yield:

$$p(t) = \sum_{k=0}^{\infty}\left\{P_{f_k}e^{i\omega_k t} + P_{b_k}e^{-i\omega_k t}\right\} \quad (36)$$

Equation (36) shows that the movement of a point in the plane can be considered as the superposition of several harmonic motions with different frequencies. Analyzing a specific node of the rotor, at a given natural frequency, it can be seen that the modal form can be expressed by:

$$p(t) = P_f e^{i\Omega t} + P_b e^{-i\Omega t} \quad (37)$$

This way, it is possible to see that the two-dimensional movement from one point of the rotor can be interpreted as a composition of two sub-modes: The first, spinning in the same direction of rotation of the rotor (forward whirl) and the second, rotating in the opposite direction (backward whirl).

Applying the complex transformation through the matrix $[T]$ to the equation of motion seen in (34) results in:

$$[M_c]\begin{Bmatrix}\ddot{p}\\ \ddot{\bar{p}}\end{Bmatrix} + [G_c(\Omega)]\begin{Bmatrix}\dot{p}\\ \dot{\bar{p}}\end{Bmatrix} + [K_c]\begin{Bmatrix}p\\ \bar{p}\end{Bmatrix} = \begin{Bmatrix}f\\ \bar{f}\end{Bmatrix} \quad (38)$$

Where:

$$[M_c] = [T]^{-1}[M][T] \quad (39)$$

$$[G_c] = [T]^{-1}[G][T] \quad (40)$$

$$[K_c] = [T]^{-1}[K][T] \quad (41)$$

Equation (38) can be placed in the form of state space equation, as seen in (42).

$$[A_c]\{\dot{x}(t)\} - [B_c]\{x(t)\} = \{f(t)\} \quad (42)$$

Where:

$$[A_c] = \begin{bmatrix}[0] & [M_c]\\ [M_c] & [G_c]\end{bmatrix} \quad (43)$$

$$[B_c] = \begin{bmatrix}-[M_c] & [0]\\ [0] & [K_c]\end{bmatrix} \quad (44)$$

$$\{x\} = \begin{Bmatrix}\begin{Bmatrix}\dot{p}\\ \dot{\bar{p}}\end{Bmatrix}\\ \begin{Bmatrix}p\\ \bar{p}\end{Bmatrix}\end{Bmatrix} \quad (45)$$

$$\{f\} = \begin{Bmatrix}\begin{Bmatrix}0\\ 0\end{Bmatrix}\\ \begin{Bmatrix}f\\ \bar{f}\end{Bmatrix}\end{Bmatrix} \quad (46)$$

Assuming external forces and harmonic displacements will yield (47) through (42).

$$(s[A_c] + [B_c])\{X\} = \{F\} \quad (47)$$

Where:

$$s = i\omega \quad (48)$$

$$\{X\} = \begin{Bmatrix}s\begin{Bmatrix}P_f\\ \bar{P}_b\end{Bmatrix}\\ \begin{Bmatrix}P_f\\ \bar{P}_b\end{Bmatrix}\end{Bmatrix} \quad (49)$$

$$\{F\} = \begin{Bmatrix}\begin{Bmatrix}0\\ 0\end{Bmatrix}\\ \begin{Bmatrix}G_f\\ \bar{G}_b\end{Bmatrix}\end{Bmatrix} \quad (50)$$

From (47), the forced response can be given by:

$$\{X\} = (s[A_c] - [B_c])^{-1}\{F\} \quad (51)$$

In the case of free vibrations:

$$(s[A_c] - [B_c])\{X\} = \{0\} \quad (52)$$

The non-symmetry of the involved matrices leads to two eigen value problems:

$$(s_i[A_c] - [B_c])\{R\}_i = \{0\} \quad (53)$$

$$\{L\}_i^T(s_i[A_c] - [B_c]) = \{0\}^T \quad (54)$$

Right and left eigen vectors are:

$$\{R\}_i = \begin{Bmatrix}\lambda_i\{r_i\}\\ \{r_i\}\end{Bmatrix} \quad (55)$$

$$\{L\}_i = \begin{Bmatrix}\lambda_i\{l_i\}\\ \{l_i\}\end{Bmatrix} \quad (56)$$

Where $\{r_i\}$ and $\{l_i\}$ are the eigen vectors on the right and left of the eigen value problem of second order, seen in (38). The inverse of the dynamic stiffness matrix can be expanded in terms of eigen vectors on the right and left, according to (57).

Table 1. Mechanical property of rotor to simulation.

Rigid Disk	
Mass (Kg)	2.46
Radius (m)	0.05
Thickness (m)	0.04
Diametral Mass Moment of Inertia (Kg.m^2)	1.87x10^{-3}
Polar Mass Moment of Inertia (Kg.m^2)	3.08x10^{-3}
Circular shaft	
Diameter (m)	8.0x10^{-3}
Length (m)	0.62
Second Moment of Inertia (Kg.m4)	0.2x10^{-9}
Young Modulus (N/m^2)	2.1x10^{11}
Density (Kg/m^3)	7850

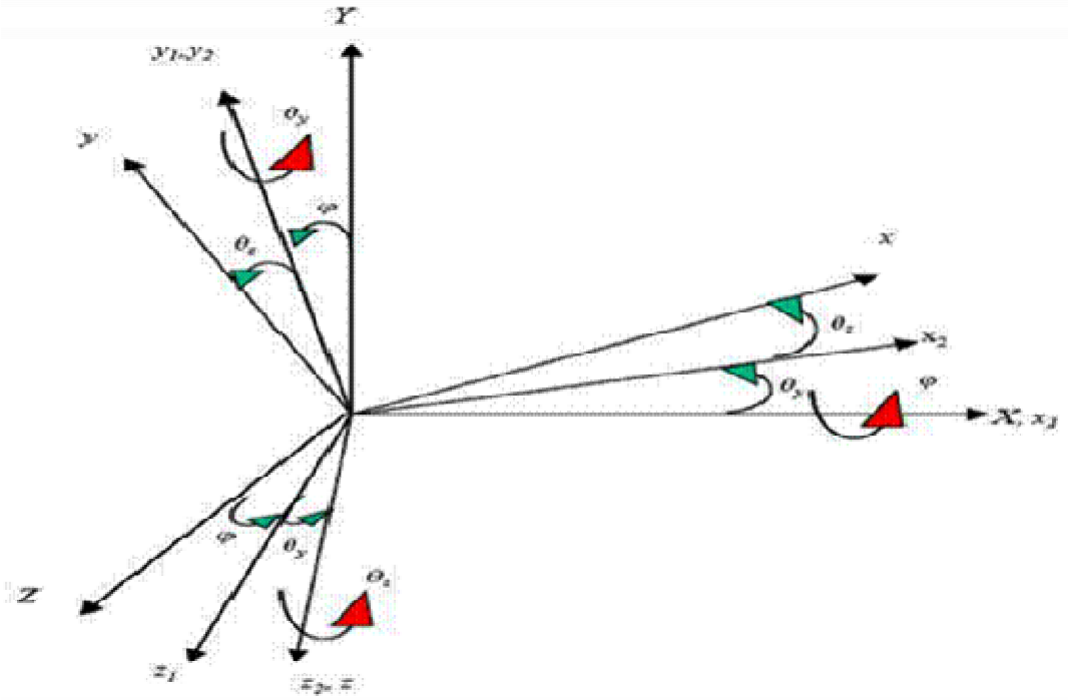

Figure 3. Rotation angles.

$$(s[A_c] - [B_c])^{-1} = \sum_{i=1}^{4n} \frac{\{R\}_i\{L\}_i^T}{s-\lambda_i} \quad (57)$$

Considering only the displacements, the frequency response for the forced system is obtained by:

$$\begin{Bmatrix}\{P_f\}\\ \{P_b\}\end{Bmatrix} = \left[\sum_{i=1}^{4n} \frac{\{r_i\}\{l_i\}^T}{i\omega-\lambda_i}\right]\begin{Bmatrix}\{G_f\}\\ \{G_b\}\end{Bmatrix} \quad (58)$$

Numerical Simulations

A computational routine was implemented using the MATLAB software. Two examples were made, one being a simple rotating shaft and the other a drill string. In the first instance it appeared to validate the system by comparing with literature. The second instance shows the possibility of using in drill strings, used in the construction of oil wells. Both examples were performed with the presentation of charts, tables and forward and backward modes, through complex modal analysis.

Example 1 – Simple rotating shaft

The Table 1 shows the input data for simulation of the vertical rotor.

The test model, shown in Figure 3, consists of an

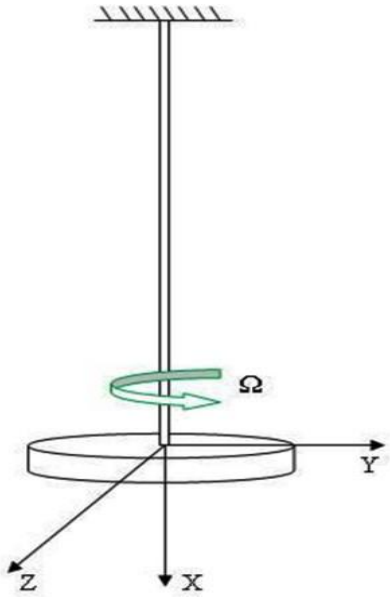

Figure 4. Schematic rotary system model to simulation.

Table 2. Critical speed and vibration modes.

Critical Speed (Hz)		Whirl Mode	Mode
ωc1	2.3	Backward	First
ωc2	2.3	Forward	First
ωc3	34.0	Backward	Second
ωc4	-	Forward	Second

elastic shaft fixed in one end and free at the other, while the disk is jointly attached to the shaft at the bottom.

The solution of the problem by the presented modeling leads to two important results for the mechanical system, the eigen values and eigen vectors. Considering the sub-damped system, the eigen values come in complex numbers, where the imaginary part indicates the natural frequency and real part of the damping factor. The eigen vectors bring about their own modes of vibration.

The rotating systems experience situations of risk when operating at certain speeds of rotation called critical speeds. The speed is considered critical when it equals any of the natural frequencies of the system, which in, depends on the speed of rotation. To find the critical speeds, one traces the natural frequencies obtained by the simulator with the speed of rotation of the disk, in this same graph, the line is drawn $\omega_n = \Omega$. The critical speeds are determined where the points $\omega_n = \Omega$ intersect the curve of natural frequencies. The diagram represented in Figure 4 displays the results obtained with the model presented in this study.

For a non rotating system (Ω = 0), the modes of vibration are composed of a bending and a rotation one. When the system turns, these two modes still exist, but each of them is separated into two, one forward and one backward. Figure 4 shows the variation of four natural frequencies, w_1, w_2, w_3 and w_4 with the speed of rotation Ω of the system, as the items of critical speed. The critical speeds w_{c1} and w_{c2} matches to the backward and forward whirl motion, respectively, in the first mode of vibration and critical speed w_{c3} match to backward whirl motion in the second mode of vibration, as numerical data presented in Table 2.

In Campbell diagram it can be seen that w_{c4} does not exist, moreover, w_{c1} and w_{c3} are in fact "false critical speeds". Therefore, there will only be the critical speed w_{c2} = 2.3 Hz of the first forward mode, Alamo (2003).

The natural frequencies w_1 and w_2 are practically on horizontal lines, it means, they vary very little with the rotation speed. This means that the gyroscopic effect is concentrated mainly in the second mode of vibration, while the first mode can be practically analyzed by a simplified model that does not include the deflections of the disk. The value of static natural frequency of the rotation system for the first mode, i.e. with zero rotation (Ω = 0) is 2.3 Hz and the second mode, the natural static

Table 3. Complex Modal Analysis Results.

Eigenvalues [rad/s]	
0 + 15.889 i	0 + 13.065 i
Natural Frequencies (Hz)	
2.54	2.09
Right vectors { Pf_1 Pf_2 Pb_1 Pb_2 }^{T}	
0.025454	3,50E-11
0.057424	8,87E-11
2,01E-13	0.027662
4,35E-13	0.071127
Whirl mode	
Forward	Backward
Orbit	
Circular	Circular

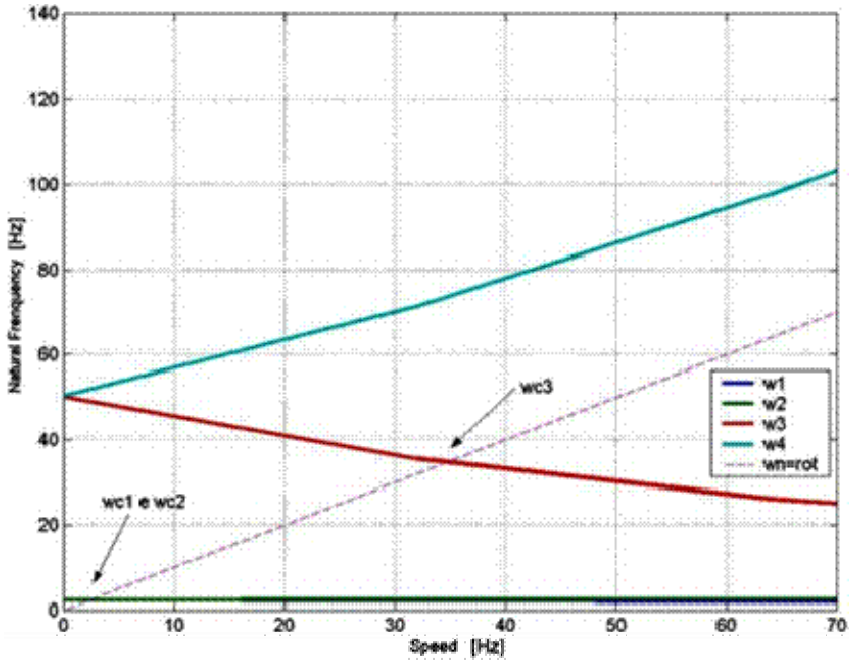

Figure 5. Campbell Diagram and critical speed.

frequency is 50 Hz.

The Table 3 shows the modal parameter obtained through the formulation of complex modal analysis for the rotor shown in Table 1 with constant rotation speed of 400 rad/s. Unlikely from what happens when it is used real coordinates in modeling, where you need to post processing the modal vectors to identify the modes of precession, the complex formulation already provides this result very clearly. For it, simply compare the modulus of forward and backward components of the modal vectors. Moreover, one can obtain the shape of the orbit. In this case, as there is no damping and rotor is isotropic, there are null values for both backward and forward whirl components.

The Figure 5 provides a comparison with the traditional and the complex modal analysis in rotor shown in Table 1 in the implementation of various rotational speeds. It can be seen the distinction between the peaks of forward and backward whirl as increasing the speed clearly in the curves of the directional frequency response function

Example 2 – Drillstring

The example of the rotor in the following study it is a drillstring, normally used in construction of oil wells.The Figure 6 shows the drillstring design with discretization.

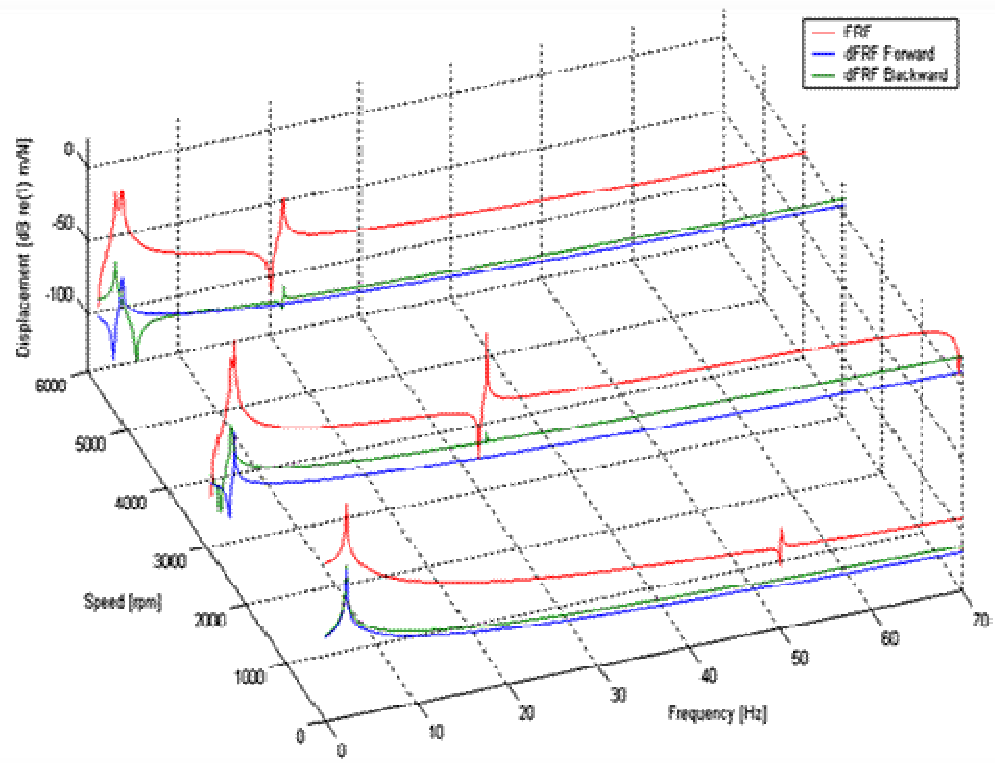

Figure 6. Classical modal analysis (FRF) and Complex modal analysis (dFRF).

Table 4. Input data for drillstring.

Element	Node	Coord X (m)	Length (m)	Internal Diameter (m)	External Diameter (m)	Drillstring element name
1	1	0	9,98	0,1086	0,127	TOP DRIVE / DP 5”
	2	1060,82				
2			1060,83	0,1086	0,127	DP 5"
	3	2121,65				
3			1060,83	0,1086	0,127	DP 5"
	4	3182,48				
4			26,76	0,0762	0,127	3 HWDP 5"
	5	3209,24				
5			84,61	0,0732	0,1715	9 DC 6.3/4"
	6	3293,85				
6			110,15	0,0762	0,127	12 HWDP 5"
	7	3404				
7			71,47	0,0762	0,2032	FS / STAB / KM / PBL / 5 DC 8" / DJAR / XO
	8	3475,47				
8			14,55	0,0488	0,2032	LWD 8" / MWD 8"
	9	3490,02				
9			9,98	0,0605	0,2446	RSS 9,63" / BIT 12.1/4”
	10	3500				

The Table 4 shows the input data for drillstring.

The Figure 7 presents the results for the frequency response function to drill string through the formulation of complex modal analysis. The finite element discretization of 30 nodes distributed in 31 elements, being composed of 354 degrees of freedom after applying boundary

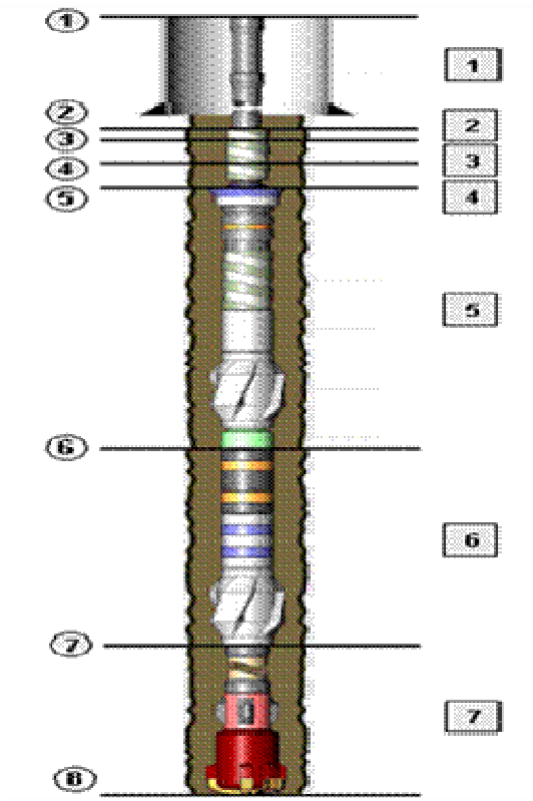

Figure 7. Drillstring design with discretization.

conditions.

We plotted frequency response function through the classical and in the same graph as plotted frequency response function by complex modal analysis method. One can see that there is a correlation between the frequency peaks in both methods. The great advantage of the complex method is to allow the clear identification of forward and backward whirl modes.

CONCLUSIONS

A dynamic formulation of rotating systems by finite element method was developed and implemented in MATLAB considering gyroscopic and gravitational effects, i.e., shaft subjected to its own weight, to study vibrations in flexible vertical rotors. The results showed good precision with respect to analytical and numerical studies drawn from the cited references. The model is limited to axi-symmetric, homogeneous, isotropic and non-linear rotors with a vertical cylinder and with one fixed end and another free. The developed system allows performing more advanced studies with long and slender shafts, as it is the usual in drill string oil wells. In this case, more detailed analysis, including dynamic effects resulting from contact with the wall of the borehole and the damping effects due to hydrostatic forces inside and outside of the pipes can be coupled to the model, thus enabling studies considering forced vibrations with response analysis in the frequency domain by complex modal analysis, aiming to investigate the modes of forward and backward whirl, which are highly damaging to rotating systems.

ACKNOWLEDGEMENTS

This research was supported by Department of Mechanical Engineering, Universidade Estadual Paulista, Bauru-SP.

REFERENCES

Alamo FJC (2003). Dinâmica de um Rotor Vertical em Balanço com Impacto, MSc Dissertation, Pontifícia Universidade Católia, Rio de Janeiro, Brazil.

Alnaser HA (2002). Finite Element Dynamic Analysis of DrillString, MSc Dissertation, King Fahd University of Petroleum and Minerals, Dhahran, Saudi Arabia.

Axisa F, Antunes J (1990). Flexural vibrations of rotors immersed in dense fluids: Part I – Theory, Proceedings of the Third International Symposium on Transport Phenomena and Dynamics of Rotating Machinery, ISROMAC-3, Honolulu, Hawaii, Vol. 2, pp. 23–38.

Bailey JR et al (2008). Drilling vibrations modeling and field validation. IADC/SPE 112650, Drilling conference held in Orlando, Florida, USA.

Bashmal SM (2004). Finite Element Analysis of Stick-slip Vibrations in

Drillstrings, Msc Dissertation, King Fahd University of Petroleum and Minerals, Dhahran, Saudi Arabia.

Bazoune A, Khulief YA (2001). A Finite Beam Element for Vibration Analysis of Rotating Tapered Timoshenko Beams, J. Sound and Vibration, Vol. 156, pp. 141-164.

Cordovil AGDP (1991). Análise Dinâmica de Colunas de Perfuração via Superposição Modal, MSc Dissertation, Universidade Estadual de Campinas, São Paulo, Brazil.

Da Silva EL (2004). Dinâmica de Rotores: Modelo Matemático de Mancais Hidrodinâmicos, MSc Dissertation, Universidade Federal do Paraná, Paraná, Brazil.

Dana SS (1987). Análise Dinâmica de Rotores com Eixo Vertical, PhD Thesis, Universidade Estadual de Campinas, São Paulo, Brazil.

Dunayevsky VA, Abbassian F, Judzis A (1993). Dynamic stability of drillstring under fluctuating weight on bit, SPE Paper No. 14329, SPE Drill, pp. 84–92.

Ewins DJ (1998). Modal Analysis for Rotating Machinery, IFToMM, Darmstadt, 1998.

Kessler CL (1999). Complex Modal Analysis of Rotating Machinery, Phd Thesis, Cincinnati University, Cincinnati.

Khulief YA, Mohiuddin MA (1997). On the dynamic analysis of rotors using modal reduction, Journal of Finite Elements in Analysis and Desing, Vol. 26, pp. 41-55.

Lee CW (1991). A Complex Modal Testing Theory for Rotating Machinery, Mechanical Systems and Signal Processing, v5, n2, p.119-137.

Mathworks, Inc. Matlab ® 7.9.0 (R2009b).

Ritto TG (2010). Numerical analysis of the nonlinear dynamics of a drill-string with uncertainty modeling, Phd Thesis, Postgraduate Program in Mechanical Engineering, Pontifícia Universidade Católica do Rio de Janeiro, Brazil.

Souto CA (2000). Estudo do Comportamento Dinâmico de Máquinas Rotativas através da Análise Modal Complexa, MSc Dissertation, Universidade Estadual de Campinas, São Paulo, Brazil.